

Observation of Magnonic Band Gaps in Magnonic Crystals with Nonreciprocal Dispersion Relation

M. Mruczkiewicz¹, E. S. Pavlov², S. L. Vysotskii², M. Krawczyk¹, Yu. A. Filimonov^{2,3}, S. A. Nikitov^{3,4,5}

¹ Faculty of Physics, Adam Mickiewicz University in Poznan, Umultowska 85, Poznań, 61-614 Poland

² Kotel'nikov Institute of Radio-Engineering and Electronics of RAS,

Saratov Branch, Zelenaya Str. 38, Saratov, 410019, Russia.

³ Saratov State University, Astrakhanskaya Str. 83, Saratov, 410012, Russia.

⁴ Kotel'nikov Institute of Radio-Engineering and Electronics of RAS,

Mokhovaya Str. 11, Bld. 7, Moscow, 125009, Russia.

⁵ Moscow Institute of Physics and Technology, Dolgoprudny, 141700, Moscow Region, Russia.

(Dated: September 5, 2022)

An effect of metallization of the magnonic crystal surface on the magnonic band gaps is studied experimentally and theoretically. The structures under investigation are one-dimensional magnonic crystals based on the yttrium iron garnet with an array of etched grooves. The shift of band gaps due to the presence of conducting overlayer was measured in transmission line experiments. The numerical calculations and model analysis give further insight into the origin of the band gaps and on the nonreciprocal dispersion relations of spin waves in metallized magnonic crystals. The calculations confirmed with experimental data show that when metal is present near one of the surface, the gap position is shifted from the border of the Brillouin zone. This positive answer to the outstanding question about possibility of existence magnonic band gaps in nonreciprocal part of the spin wave spectra in metallized magnonic crystals creates potential for new applications and improvements of already existing prototype magnonic devices.

The spin wave (SW) propagating in a ferromagnetic film along the perpendicular direction to a tangentially applied magnetic field (in Damon-Eschbach geometry)¹ possesses a nonreciprocal character. More specifically, a distribution of an amplitude of spin wave is nonsymmetric across the thickness, d , of the film. The degree of SW localization strongly depends on the value of its wavenumber k . For sufficiently large wavevectors the localization of the amplitude near one of the edge is present, which depends upon the direction of propagation and direction of the external magnetic field. It was shown that applying a metal overlayer on one side of the film affects strongly only the spin wave propagating in one direction.^{2,3} As a result of the metallization the nonreciprocal dispersion relation appears: $f(k) \neq f(-k)$, where f is a frequency.⁷ However, the amplitude localization and the nonreciprocity depends on the wavenumber, film thickness and its separation from the metallic film.

Since magnonic crystals (MCs) bring wide attention of researchers due to its usefulness for manipulation of spin wave band structure,⁴⁻⁸ it is natural that the influence of metallization on MCs was also recently investigated. It was shown experimentally that the band gap at frequency of unmetallized structure disappears when the metal is attached.⁹ However, as yet the predictions of numerical calculations that the gaps appear at higher frequency range were not demonstrated experimentally.^{10,11} Here we present an experimental demonstration of the nonreciprocal dispersion relation of spin waves and existence of an indirect magnonic band gap in one dimensional magnonic crystals in contact with the metallic film.

The nonreciprocal properties of magnonic band structure are potentially useful to design miniaturized mi-

crowave isolators and circulators, essential elements in microwave technology. The structure based on the uniform yttrium iron garnet (YIG) film with metallic stripes was proposed as a ultrasensitive magnetic field sensors.¹² Although nonconsidered in that study, the nonreciprocal properties of SW can influence positively their sensitivity. The nonreciprocity can be also of big importance for magnonics, where spin waves are used to process information.^{13,14} The dispersion metal-YIG structures is also an important factor for electrically tunable magnonic device.¹⁵ The technologically simple design proposed here can be of advance over other complicated magnonic crystal based nonreciprocal structures.¹⁶ Moreover, the influence of metal in the surrounded space of a magnonic device, especially when integrated, can additionally result in changes of its functionality.^{17,18}

Here, we investigate an influence of a metal on the magnonic band structure in two microscale MCs made of YIG films with etched grooves. The structure under consideration is depicted in Fig. 1. The YIG films were grown on the $\langle 111 \rangle$ -oriented gadolinium gallium garnet (GGG) substrate. The grooves were introduced by chemical etching on the YIG surface, which form a periodic structurization. The first MC (Sample I) consists of the $7.7 \mu\text{m}$ thick YIG film with an array of etched grooves of the depth $g = 1.5 \mu\text{m}$ and width $w = 80 \mu\text{m}$. The separation between grooves is $70 \mu\text{m}$ and the lattice constant is of $a = 150 \mu\text{m}$. The second MC (Sample II) is the $3.8 \mu\text{m}$ thick YIG film with an array of grooves with the depth: $g = 2 \mu\text{m}$ and the width: $w = 50 \mu\text{m}$. The separation between grooves is $150 \mu\text{m}$ and the lattice constant is of $a = 200 \mu\text{m}$. The wavevectors at the edge of the first BZ for the investigated structures are 2×10^4 1/m and 1.5×10^4 1/m, for the sample I and II, respec-

tively. On the basis of the analysis conducted in Ref. [?] we can expect that for chosen lattice constant the effect of metallization ought to be observable if dielectric spacer between MC surface and metal screen (see Fig. 1) have thickness $t \approx 100 \mu\text{m}$ (i.e., or smaller than a). On the other hand the air gap of such values can be easily realized experimentally.^{19,20}

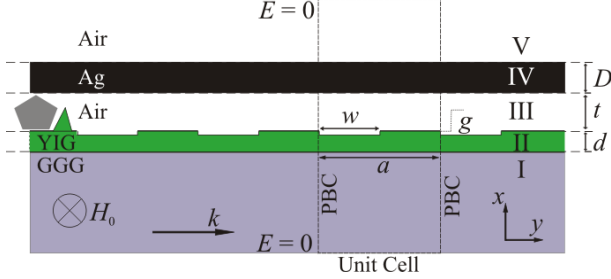


FIG. 1. (Color online) A schema of the structure under consideration. The materials are indicated as follows: I) dielectric substrate (GGG), II) magnonic crystal (YIG), III) air gap, IV) metallic overlayer (Ag) and V) air surrounding. The bias magnetic field H_0 is in the film plane and directed along the z axis. The SWs propagate along the y axis. The rectangular unit cell used in numerical calculations is marked by dashed line. The periodic boundary conditions (PBC) were used along the x axis. The bottom and top border of the unit cell is far from the structure, at these borders we assume fields equal 0.

To measure transmission and phase characteristic of SWs MCs were placed on two types of delay lines, coplanar and microstrip waveguides (Fig. 2), on input and output transducers of the width $w_T \approx 30 \mu\text{m}$ and length of $l_T = 4 \text{ mm}$. The two transducers were separated by a distance $L_T = 4 \text{ mm}$. The YIG films under investigations had planar dimensions $15 \text{ mm} \times 5 \text{ mm}$. The whole structure was placed in the gap of an electromagnet so that the external magnetic field was oriented along the grooves and parallel to the transducers. The field was strong enough to saturate the sample ($\mu_0 H_0 = 41.6 \text{ mT}$). The amplitude-frequency (AF) and phase-frequency (PF) characteristics of the delay line prototype models were measured by an Agilent E5071C-480 network analyzer. The ground layer of metal of the coplanar line is of thickness $D = 5 \mu\text{m}$ and it is in close with the MC. This ground layer serves also as a metal overlayer depicted in Fig. 1.

Using those two different types of delay lines (microstrip and coplanar) the transmission of SWs in MC without and with a metallic overlayer were measured for Sample I and II. The measured transmission spectra (AF characteristic) are shown in Figs. 3(a) and (c) and in Figs. 5(a) and (c) for Sample I and II, respectively. Magnonic band gaps indicated by low AF signal

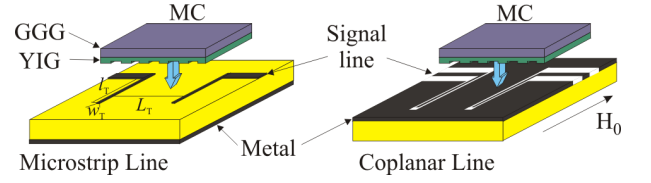


FIG. 2. (Color online) A microstrip (left) and coplanar (right) line used in the SW transmission measurements through MC without and in contact with metallic overlayer. In the experimental setup MC sample is placed atop with grooves side close to the transducers.

are found in both transmission spectra and marked by shadowed rectangles. However, in the case of MCs with metallic overlayer (Figs. 3(c) and 5(c)) the first magnonic gap is shifted to the higher frequencies on some values Δf , see Fig. 3(e) and Fig. 5(e). The frequency shift was $\Delta f \approx 120 \text{ MHz}$ and $\Delta f \approx 140 \text{ MHz}$ for samples I and II, respectively. The existence of these gaps is confirmed also in the respective PF characteristics which are presented in Figs. 3(b) and (d) and Figs. 5(b) and (d) for Sample I and II, respectively.

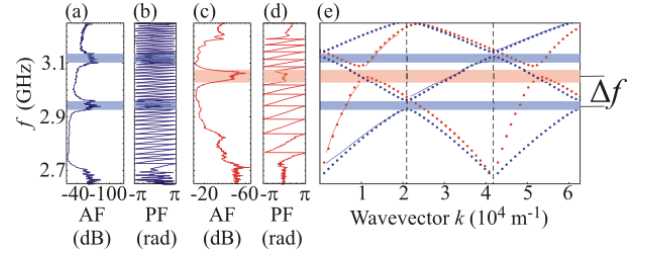


FIG. 3. (Color online) Result of the measurements for Sample I ($a = 150 \mu\text{m}$). a) Amplitude-Frequency (AF), b) Phase-Frequency (PF) characteristics of YIG MC without metal overlayer, c) AF and d) PF characteristics of YIG MC with metal overlayer. e) The comparison of dispersion relation obtained from numerical calculations (blue dots for unmetallized sample, red dots for metallized) and from measured PF signal (blue lines for unmetallized sample and red lines for metallized). The transparent blue and red bars indicate experimentally measured positions of magnonic band gaps in unmetallized and metallized sample, respectively. The vertical dashed lines in (e) indicate the edges of Brillouine zones and Δf is the frequency shift of the magnonic gap induced by metallization.

In order to obtain more insight into the formation of the magnonic band gaps in the nonreciprocal structure the numerical calculations of the dispersion relation were performed. For SWs from the GHz frequency range, a large value of thickness of MCs considered in the paper and a small value of exchange constant of YIG the magnetostatic approximation is well justified. Therefore, the exchange coefficient in YIG is neglected in our theoretical investigation. In order to calculate the SW dispersion

relation we solved the wave equation for an electric field vector \mathbf{E} :²¹

$$\nabla \times \left(\frac{1}{\hat{\mu}_r(\mathbf{r})} \nabla \times \mathbf{E} \right) - \omega^2 \sqrt{\epsilon_0 \mu_0} \left(\epsilon_0 - \frac{i\sigma}{\omega \epsilon_0} \right) \mathbf{E} = 0, \quad (1)$$

where $\omega = 2\pi f$, μ_0 and ϵ_0 denote the vacuum permeability and permittivity, respectively, and σ is the conductivity, different from zero only in the metallic overlayer. To describe the dynamics of the dynamic magnetization components perpendicular to the external magnetic field, it is sufficient to solve the Eq. 1 for the z component of the electric field vector \mathbf{E} which depends solely on x and y coordinates⁷: $E_z(x, y)$. The MCs under consideration are assumed infinite along the z direction. The permeability tensor $\hat{\mu}(\mathbf{r})$ is obtained from the linearized damping-free Landau-Lifshitz equation:²²

$$\hat{\mu}_r(\mathbf{r}) = \begin{pmatrix} \mu^{xx}(\mathbf{r}) & i\mu^{xy}(\mathbf{r}) & 0 \\ -i\mu^{yx}(\mathbf{r}) & \mu^{yy}(\mathbf{r}) & 0 \\ 0 & 0 & 1 \end{pmatrix}, \quad (2)$$

where

$$\mu^{xx}(\mathbf{r}) = \frac{\gamma\mu_0 H_0 (\gamma\mu_0 H_0 + \gamma\mu_0 M_S(\mathbf{r})) - (2\pi f)^2}{(\gamma\mu_0 H_0)^2 - (2\pi f)^2}, \quad (3)$$

$$\mu^{xy}(\mathbf{r}) = \frac{\gamma\mu_0 M_S(\mathbf{r}) 2\pi f}{(\gamma\mu_0 H_0)^2 - (2\pi f)^2}, \quad (4)$$

$$\mu^{yx}(\mathbf{r}) = -\mu^{xy}(\mathbf{r}), \quad \mu^{yy}(\mathbf{r}) = \mu^{xx}(\mathbf{r}); \quad (5)$$

M_S is the saturation magnetization of YIG and γ is the gyromagnetic ratio. Eq. (1) has coefficients being constants or periodic function of y (with a period a), thus the Bloch theorem can be used:

$$E_z(x, y) = E'_z(x, y) e^{ik_y y}, \quad (6)$$

where $E'_z(x, y)$ is a periodic function of y : $E'_z(x, y) = E'_z(x, y + a)$. k_y is a wave vector component along y and due to considering SW propagation along this direction only we assume $k_y \equiv k$. Eq. (1) together with Eq. (6) can be written in the weak form²³ and the eigenvalue problem can be generated. This eigenequation is supplemented with the Dirichlet boundary conditions at the borders of the computational area placed far from ferromagnetic film along x axis (dashed lines in Fig. 1). This eigenequation is solved by the finite element method with the use of a commercial COMSOL software.

In calculations we take nominal values of the MC dimensions (for Sample I and II) and the saturation magnetization of YIG as $M_S = 0.143 \times 10^6$ A/m and $M_S = 0.142 \times 10^6$ A/m for Sample I and II, respectively. Note the difference in M_S can be attributed to growth anisotropy fields which results from YIG and GGG lattice mismatch during epitaxy. The conductivity of the metal is assumed as $\sigma = 6 \times 10^7$ S/m, which is a tabular value for Ag.

Because the MC was putted just on the top of the transducers without any polishing of the MC surface, the real separation can be in the range of few to dozen μm

due to some irregularities or dust grains (schematically shown in Fig. 1). In addition, any irregularity of YIG film or a metal layer will also results in an increase of this separation. It is also possible that conductivity of the metal σ or its thickness D is lower than assumed in the calculations. However, the dispersion relation is not sensitive for variation of the product of conductivity and thickness of the metal, σD at a range of SW wavenumbers in the interest.²⁴ Thus only the t was used as a free parameter in calculations. In Fig. 4 the frequency shift (Δf) of the first magnonic band gap in the Sample I with the metallic overlayer with respect to the MC without the metal is shown in dependence on t . There is a monotonous decrease of Δf with increasing t , because the influence of the metal decreases. The agreement with the experimental data for Sample I with the metallic overlayer is achieved for $t = 18 \mu\text{m}$ and this value is used in the following calculations.

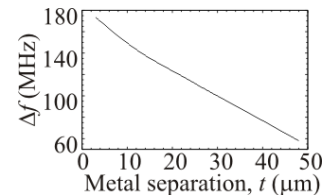


FIG. 4. The metallization induced frequency shift (Δf) of the magnonic band gap in Sample I in dependence on the separation distance of the metal from the magnonic crystal surface.

In Fig. 3 (e) the results of calculated dispersion relation are presented by blue and red dots for Sample I without and with metallic overlayer, respectively. In this figure we can see that the edge of the magnonic band gap in the metallized structure is shifted from the border of the Brillouin zone and this effect is due to nonreciprocity of the SW dispersion relation. The gap opens when the interacting SWs with equal frequencies fulfill the general Bragg condition.¹¹ Magnonic band gaps are marked by transparent blue and red horizontal bars for measurements with and without metallic overlayer, respectively. The size of the first magnonic gap is 39 MHz for sample with metal overlayer and 35 MHz for sample without metal overlayer. The position and the width of the band gaps from calculations agree very well with the gaps found in the transmission experiment. Thus, we have shown experimentally that magnonic band gaps can exist in MCs covered by a metallic overlayer in the frequency and wavevector part of the SW spectra where nonreciprocal properties are significant.

From the measured PF characteristic we can obtain even more information about the SW dispersion in MCs than from the AF characteristic. The PF graphs are reduced to the $-\pi$ and π values and of course the waves with phase difference 2π are not differentiable. But the

phase jump over 2π phase difference visible in the PF characteristic at frequencies from a transmission band is determined by the separation distance between the transducers and is related to the change of the SW wavevector $\Delta k = 2\pi/L_T = 0.157 \times 10^4 \text{ m}^{-1}$. This way the dispersion relation can be estimated, although ambiguously it gives a clear information about the slope of the dispersion curve (i.e., its group velocity) at different parts of the magnonic spectra. Comparing Fig. 3 (b) and (d) we can see that the group velocity of SWs from the first and second band in MC with metal are much higher than respective velocities in MC without a metal. By assigning a wavevector $k = n\pi/a$ for the frequency corresponding to the value of phase equal to $-\pi$ at the edge of the n -th magnonic gap we can superimpose the function $f(k)$ extracted from PF characteristic on the calculated dispersion relation. These dispersions are presented with red and blue continuous lines in Fig. 3(e) for Sample I. The agreement between measured and calculated dispersion curves is very good and proves that the metallic overlayer can be used not only to tune position of the magnonic band gap but also to mold the velocity of the transmitted signal. Moreover, the shape of the dispersion curve at the magnonic band gap edge can be important factor for possible applications of MCs, e.g., as ultrasensitive sensors of a magnetic field.¹²

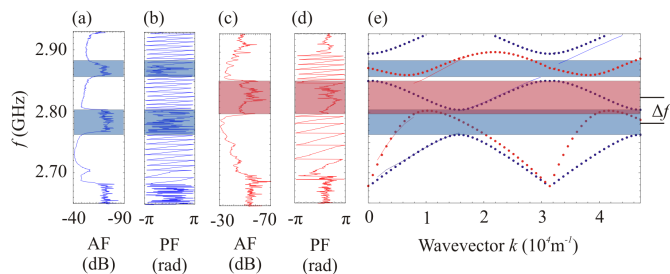


FIG. 5. (Color online) The result of measurements and calculations for Sample II ($a = 200 \mu\text{m}$). (a) AF and (b) PF characteristics of YIG MC without metal overlayer; (c) AF and (d) PF characteristics of YIG MC with metal overlayer. (e) The comparison of dispersion relation obtained from numerical calculations (blue dots for unmetallized sample, red dots for metallized) and from PF signal (blue line for unmetallized sample, red line for metallized). The transparent blue and red bars indicate experimental positions of the magnonic band gaps in unmetallized and metallized sample, respectively.

Fig. 5 (a)-(d) shows a results of measured AF and PF characteristics of unmetallized and metallized Sample II ($a = 200 \mu\text{m}$ and width of the grooves $w = 50 \mu\text{m}$). The comparison of dispersion relations extracted from the PF characteristics with the results of calculations is shown in Fig. 5 (e). In this case the separation between YIG and metal was taken as $t = 28 \mu\text{m}$. The AF and PF characteristics show wide band gaps (wider than for Sample I) at different frequency ranges. The size of the first

magnonic gap is 61 MHz for sample with metal overlayer and 44 MHz for sample without metal overlayer. It is due to the larger ratio of groove depth to YIG thickness. Again, band gap at elevated frequencies is measured with the use of coplanar lines. The numerical dispersion relation confirm existence of a large indirect magnonic band gap and a larger group velocity of SWs in the Sample II with agreement with the dispersion extracted from the PF characteristic.

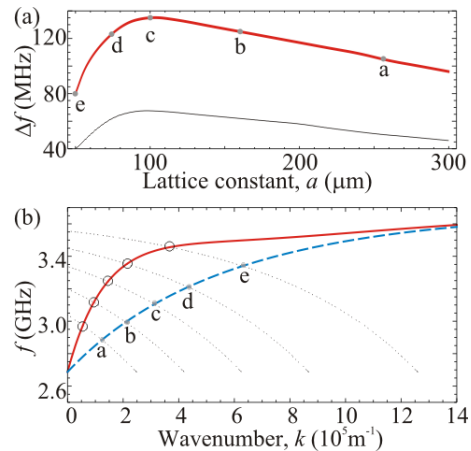


FIG. 6. (Color online) (a) Shift of the magnonic band gap frequency due to metallization as a function of the lattice constant. The thick red solid line is for YIG MC of $7.7 \mu\text{m}$ thickness and $1.5 \mu\text{m}$ deep grooves with the width of $w = 0.5a$. The black thin line is for YIG MC of thickness $3.8 \mu\text{m}$ and $2 \mu\text{m}$ deep grooves with the width of $w = 0.25a$. The separation of metal layer from MC was fixed to $18 \mu\text{m}$ in both cases. (b) The SW dispersion relation of a homogeneous YIG film of $7.7 \mu\text{m}$ thickness with a metal overlayer (red solid line) and without metal (blue dashed line). The gray dotted lines are artificially introduced back-folded branches due to selected periodicities marked in (a) by letters from a to e. The small full-gray and big empty dots indicate the expected positions of the magnonic band gap in MC without (which opens at the border of the first Brillouin zone, π/a) and with metallic overlayer (inside the Brillouin zone), respectively, for selected lattice constant in (a).

Additional calculations were performed to find influence of the lattice constant on the shift of the frequency of the magnonic band gap due to metallization. The frequency of the band gap shift in dependence on the lattice constant for YIG MC of $7.7 \mu\text{m}$ thickness and $1.5 \mu\text{m}$ deep grooves with the width of $w = 0.5a$ is shown with bold solid red line in Fig. 6 (a). The same function is also plotted for MC of thickness $3.8 \mu\text{m}$ and $2 \mu\text{m}$ deep grooves of the width $w = 0.25a$ with thin gray line. In both cases the separation of metal from MC surface was fixed to $18 \mu\text{m}$. It can be seen that for MCs characterized by different thicknesses it is possible to define an optimal value of the lattice constant for which the shift of the band gap is largest.

The dependance in Fig. 6 (a) can be understood by analysis of the dispersion relation of SWs in a homogeneous YIG film shown in Fig. 6 (b), where the solid-red and blue-dashed lines point at the film with and without metallic overlayer, respectively. The position of the band gap in MC can be estimated by introducing artificial periodicity into homogeneous film and the exploitation of the band periodicity in the wavevector space according with the Bloch theorem. Therefore, the thin-dotted lines in Fig. 6 (b) show dispersion relations of SW propagating in the $-k$ direction (i.e., unaffected by the metal film) shifted by the reciprocal lattice vector $2\pi/a$ for five selected lattice constants marked by letters a to e in Fig. 6 (a). The small full-dots indicate the first Brillouin zone boundary (and the location of magnonic band gap in MC without metal) for chosen lattice constants; the big empty-dots point at the intersections of dispersion for $+k$ (solid red) with $-k + 2\pi/a$ (i.e., the expected location of the magnonic band gaps) for the metallized MC. The observed increase of the band gap shift with decreasing lattice constant from $a = 300 \mu\text{m}$ to $100 \mu\text{m}$ (points a, b, c in Fig. 6 (a)) is because of increasing nonreciprocity (i.e., an increase of the difference between the red-solid and dashed-blue line in Fig. 6 (b)). However, for lattice constants smaller than $a = 100 \mu\text{m}$ a decrease of the band gap shift is observed although the nonreciprocity is still meaningful close to $100 \mu\text{m}$. This is due to two effects. The first is the decrease of the nonreciprocity of the dispersion relation due to the finite conductivity and finite separation of the metal overlayer. The second is a decrease of the group velocity of the magnonic branch that is not affected by the metal. For MCs with lattice

constant smaller than $a = 73 \mu\text{m}$ (point d in Fig. 6) the shift is decreasing rapidly, since the nonreciprocity effect disappears at large wavevectors. Thus, we can conclude that the maximal shift of the frequency band gap due to contact with the metallic film is at a for which the first Brillouin zone boundary (π/a) is close to the wavenumber value where in homogeneous YIG film the nonreciprocity is largest.

In summary, we have measured the transmission of spin waves in the one-dimensional YIG based magnonic crystal. We have proved experimentally in agreement with the numerical calculations that magnonic band gaps can exist in magnonic crystals possessing nonreciprocal dispersion relation in the Damon-Eshbach geometry, i.e., for surface magnetostatic waves in which the spin wave amplitude is localized at only one surface in dependence on the direction of propagation. The numerical calculations confirmed by measured phase characteristic shows also that in this case the indirect gap is present for wavelengths which do not correspond to the periodicity.

ACKNOWLEDGMENTS

We acknowledge the financial assistance from the European Community, Grant No. FP7/2007-2013 under GA 247556 (People) NoWaPhen, from the National Science Centre of Poland, Project DEC-2-12/07/E/ST3/00538, from the Russian Foundation for Basic Research (13-07-00941-a, 14-07-00896-a and 13-07-12421-ofi-m) and from the Grant of the Government of the Russian Federation (Contract No. 11.G34.31.0030).

-
- ¹ R. W. Damon and J. R. Eshbach, "Magnetostatic modes of a ferromagnet slab," *J. Phys. Chem. Solids*, vol. 19, p. 308, 1961.
 - ² S. R. Seshadri, "Surface magnetostatic modes of a ferrite slab," *Proceedings of the IEEE*, vol. 58, p. 506, 1970.
 - ³ R. E. De Wames and T. Wolfram, "Characteristics of magnetostatic surface waves for a metalized ferrite slab," *J. Appl. Phys.*, vol. 41, p. 5243, 1970.
 - ⁴ M. Krawczyk and H. Puzkarski, "Magnonic spectra of ferromagnetic composites versus magnetization contrast," *Acta Phys. Polon. A*, vol. 93, p. 805, 1998.
 - ⁵ S. Neusser, B. Botters, and D. Grundler, "Spin wave modes in antidot lattices: Localization, confinement, and field-controlled propagation," *Phys. Rev. B*, vol. 78, p. 087825, 2008.
 - ⁶ S. Tacchi, B. Botters, M. Madami, J. W. Klos, M. L. Sokolovskyy, M. Krawczyk, G. Gubbiotti, G. Carlotti, A. O. Adeyeye, S. Neusser, and D. Grundler, "Mode conversion from quantized to propagating spin waves in a rhombic antidot lattice supporting spin wave nanochannels," *Phys. Rev. B*, vol. 86, p. 014417, Jul 2012.
 - ⁷ M. Krawczyk and D. Grundler, "Review and prospects of magnonic crystals and devices with reprogrammable band structure," *J. Phys.: Cond. Matter*, vol. 26, no. 12, p. 123202, 2014.
 - ⁸ A. Barman and A. Haldar, "Time-domain study of magnetization dynamics in magnetic thin films and micro- and nanostructures," *Solid State Physics*, vol. 65, p. 1, 2014.
 - ⁹ E. N. Beginin, Y. A. Filimonov, E. S. Pavlov, S. L. Vysotskii, and S. A. Nikitov, "Bragg resonances of magnetostatic surface spin waves in a layered structure: Magnonic crystal-dielectric-metal," *Appl. Phys. Lett.*, vol. 100, no. 25, p. 252412, 2012.
 - ¹⁰ M. L. Sokolovskyy, J. W. Klos, S. Mamica, and M. Krawczyk, "Calculation of the spin-wave spectra in planar magnonic crystals with metallic overlayers," *J. Appl. Phys.*, vol. 111, no. 7, p. 07C515, 2012.
 - ¹¹ M. Mruczkiewicz, M. Krawczyk, G. Gubbiotti, S. Tacchi, Y. A. Filimonov, D. V. Kalyabin, I. V. Lisenkov, and S. A. Nikitov, "Nonreciprocity of spin waves in metallized magnonic crystal," *New J. Phys.*, vol. 15, p. 113023, 2013.
 - ¹² M. Inoue, A. Baryshev, H. Takagi, P. B. Lim, K. Hatafuku, J. Noda, and K. Togo, "Investigating the use of magnonic crystals as extremely sensitive magnetic field sensors at room temperature," *Appl. Phys. Lett.*, vol. 98, no. 13, p. 132511, 2011.
 - ¹³ V. V. Kruglyak, S. O. Demokritov, and D. Grundler, "Magnonics," *J. Phys. D: Appl. Phys.*, vol. 43, no. 26,

- p. 264001, 2010.
- ¹⁴ A. Khitun, M. Bao, and K. L. Wang, “Magnonic logic circuits,” *J. Phys. D: Appl. Phys.*, vol. 43, no. 26, p. 264005, 2010.
 - ¹⁵ X. Zhang, T. Liu, M. E. Flatté, and H. X. Tang, “Electric-field coupling to spin waves in a centrosymmetric ferrite,” *Phys. Rev. Lett.*, vol. 113, p. 037202, Jul 2014.
 - ¹⁶ R. Verba, V. Tiberkevich, E. Bankowski, T. Meitzler, G. Melkov, and A. Slavin, “Conditions for the spin wave nonreciprocity in an array of dipolarly coupled magnetic nanopillars,” *Appl. Phys. Lett.*, vol. 103, no. 8, p. 082407, 2013.
 - ¹⁷ A. V. Chumak, V. S. Tiberkevich, A. D. Karenowska, A. A. Serga, J. F. Gregg, A. N. Slavin, and B. Hillebrands, “All-linear time reversal by a dynamic artificial crystal,” *Nature Comm.*, vol. 1:141, p. 1, 2010.
 - ¹⁸ S. Nikitov, S. Vysotskij, A. Dzhumaliev, E. Pavlov, Y. Filimonov, and Y. Khivintsev, “Microwave modulator on surface magnetostatic waves,” *RU2454788(C1)*.
 - ¹⁹ S. Vysotskii, E. Beginin, S. Nikitov, E. Pavlov, and Y. A. Filimonov, “Effect of ferrite magnonic crystal metallization on bragg resonances of magnetostatic surface waves,” *Technical Physics Letters*, vol. 37, no. 11, pp. 1024–1026, 2011.
 - ²⁰ S. Vysotskii, S. Nikitov, E. Pavlov, and Y. A. Filimonov, “Bragg resonances of magnetostatic surface waves in a ferrite-magnonic-crystal-dielectric-metal structure,” *Journal of Communications Technology and Electronics*, vol. 58, no. 4, pp. 347–352, 2013.
 - ²¹ G. Raju, *Antennas and Wave Propagation*. Pearson Education, 2006.
 - ²² A. Gurevich and G. Melkov, *Magnetization oscillations and waves*. CRC Press, Boca Raton, 1996.
 - ²³ M. Schäfer, *Computational Engineering - Introduction to Numerical Methods*. Springer, 2006.
 - ²⁴ Y. Filimonov and Y. Khivintsev, “Interaction between a magnetostatic surface wave and bulk elastic waves in a metallized ferromagnet-dielectric structure,” *Journal of communications technology and electronics*, vol. 47, no. 8, p. 38, 2002.